Utility of ocean wave parameters for improving predictions of ambient noise

W. Erick Rogers
Ocean Sciences Division
Naval Research Laboratory
Stennis Space Center, MS, USA
erick.rogers@nrlssc.navy.mil

Laurie T. Fialkowski
Acoustics Division, Naval
Research Laboratory
Washington, DC, USA
laurie.fialkowsi@nrl.navy.mil

Joseph M. Fialkowski
Acoustics Division, Naval
Research Laboratory
Washington, DC, USA; retired.

Daniel J. Brooker
Acoustics Division, Naval
Research Laboratory
Washington, DC, USA
daniel.brooker@nrl.navy.mil

Gleb Panteleev
Ocean Sciences Division
Naval Research Laboratory
Stennis Space Center, MS, USA
gleb.panteleev@nrlssc.navy.mil

***Abstract*—** This study is concerned with prediction of the "wind noise" component of ambient noise (AN) in the ocean. It builds on the seminal paper by [1], in which the authors quantified the correlation between AN and individual wind/wave parameters. Acoustic data are obtained from hydrophones deployed in the north and northeast Pacific Ocean, and wind/wave parameters are obtained from moored buoys and numerical models. We describe a procedure developed for this study which isolates the correlation of AN with wave parameters, independent of mutual correlation with wind speed (residual correlation). We then describe paired calibration/prediction experiments, whereby multiple wind/wave parameters are used simultaneously to estimate AN. We find that the improvement from inclusion of wave parameters is robust but modest. We interpret the latter outcome as suggesting that wave breaking responds to changes in local winds quickly, relative to, for example, total wave energy, which develops more slowly. This outcome is consistent with prior knowledge of the physics of wave breaking, e.g. [2]. We discuss this in context of the time/space response of various wave parameters to wind forcing.

***Keywords*—**ocean waves, ambient noise, wave breaking, bubbles, Wenz curves

I. Introduction

The goal of this study is to improve prediction of the component of ocean ambient noise (AN) commonly referred to as "wind noise". Important early work on this topic was performed by [3] and [4]. In these works, it was recognized that the sea state ("surface agitation") has a central role in the creation of this noise, while the underlying mechanisms were imprecisely ascribed to some combination of the action of bubbles in the water and/or the impact of sea spray on the surface. Ref. [5] argued that the latter was a dominant mechanism, but by the end of the decade, there was general recognition that bubbles play the more important role (e.g., [6], [7]). Ref. [6] outlined three frequency regimes: 1) low frequencies, 100 to 200 Hz, where bubbles in the water act as amplifiers of "water turbulence noise", 2) intermediate frequencies, 200 Hz to 1 or 2 kHz, where we tend to have a broad maximum in the wind/wave noise, caused by "collective oscillation of bubble clouds", and 3) high frequencies, 1 or 2 kHz to around 10 kHz, where individual bubble oscillation dominates. The last regime is the most well understood: this noise is emitted immediately (e.g. 10s of milliseconds) after the bubbles are formed, and the frequency of the emission is directly related to the bubble radius.

It is generally understood that wave breaking is the link between wind speed and bubble generation. Further, [8] established that the third noise mechanism above is a direct result of wave breaking. However, in the real ocean, wave breaking is not a simple function of wind speed. While wind speed is of primary importance, the frequency and intensity of wave breaking is affected by other environmental factors, e.g. see review by [2]. Consider, as illustration, an idealized case of 15 m/s wind speed over 100 m basin vs. the same wind over 100 km basin. The oceanographic difference (specifically, fetch) will result in different strength of breaking, and therefore different acoustic emissions for these two cases. Current AN models use wind speed, plus water depth (usually binary, i.e. deep vs. shallow, [4]) and/or receiver depth [9] and predict AN as a function of frequency. Our hypothesis is that since the AN is more directly connected to wave breaking than to wind speed, then it should be possible to improve a prediction of wind noise by incorporating oceanographic information.

The above hypothesis is not new. It was central to the landmark study of [1], who quantified the correlation between AN and several wind/wave parameters for a relatively short (10-

This work was funded by the Office of Naval Research via the NRL Core Program.

day) field experiment, looking at three frequencies, from 4.3 to 14 kHz. They found that the AN correlation with predicted wave dissipation rate is equal to, or slightly higher, than the correlation with wind speed. In the present study, we perform similar analysis, though here we apply multiple input parameters simultaneously to predict AN, rather than one parameter at a time. Further, we use a larger dataset: the cumulative duration of our dataset is 681 days, making it 68 times larger than that of [1], and a much broader range of frequencies are studied (127 Hz - 18 kHz, vs. 4.3 – 14 kHz).

In Section II, we present an idealized example of wave growth, to illustrate the uncertainty around the behavior of emitted AN as a type of "wave parameter". In Section III, we introduce the datasets used in the study. In Section IV, we present an analysis in which we study the correlation of AN with wave parameters, after the correlation with wind speed is removed. In Section V we perform multi-linear regression to predict AN using combined wind and wave parameters, and quantify the benefit of including wave parameters in terms of RMS error in dB. In Section VI, we discuss limitations and future work, and in Section VII, we summarize our conclusions from this study.

II. Idealized case, fetch-dependence

As in the thought experiment in Section 1, it is self-evident that for an idealized fetch-limited case, AN should grow with fetch. However, this is merely a qualitative relation, and so it does not assist us in predicting AN. A numerical ocean wave model such as SWAN (Simulating WAves Nearshore, [10]) can be used to predict many different wave parameters, each of which is associated with wave breaking to a greater or lesser degree. Table 1 show SWAN results for an idealized case with a 10-meter wind speed of 15 m/s.

TABLE I. Output from SWAN model for idealized case of wind speed of 15 m/s. Percentages shown are "percent relative to fetch of 300 km"

fetch length	300 m	3 km	30 km
fetch (%)	0.1%	1.0%	10.0%
$H_{sig}^{0.25}$	46.2%	61.2%	83.1%
$H_{sig}^{0.5}$	21.4%	37.4%	69.0%
H_{sig}	4.6%	14.0%	47.7%
T_p	17.7%	34.7%	61.8%
D_{tot}	14.7%	40.1%	95.6%
m_{-1}	0.0%	0.6%	14.2%
m_0	0.2%	1.9%	22.7%
m_1	0.9%	5.7%	35.5%
m_2	3.9%	15.2%	53.0%
m_3	13.4%	34.6%	72.7%
m_4	32.1%	61.2%	88.2%
m_5	54.2%	83.7%	95.6%
AN	unknown	unknown	unknown

Parameters given in Table 1 include moments of the wave energy density spectrum $E(f)$. They are computed as $m_n = \int_{f_1}^{f_2} E(f) f^n df$, where f_1 and f_2 are the upper and lower frequency bounds. Spectral moments typically have a physical relevance. For example, the significant waveheight H_{sig} is defined as $H_{sig} = 4\sqrt{m_0}$; m_2 is proportional to surface orbital velocity; m_3 is proportional to surface Stokes drift; m_4 is proportional to mean square slope of the sea surface; and m_5 is associated with the Phillips saturation level [11], sometimes taken as a basis for a breaking threshold [12]. D_{tot} is the integrated rate of dissipation of wave energy by whitecapping (deepwater breaking), and T_p is peak period.

The wave parameters grow at a markedly different rate. For example, D_{tot}, m_4 and m_5 grow very quickly with fetch, while total energy (m_0) grows more slowly. For the "wave parameter" AN, the growth rate is unknown, though intuition would suggest a growth rate similar to D_{tot}, m_4 and m_5. And of course, it must be recognized that even this unknown idealized growth rate of AN is likely frequency-dependent.

III. Datasets

This study relies on three datasets: 1) hydrophone observations of ambient noise, 2) observed wind/wave parameters, and 3) modeled wind/wave parameters. Each is described below.

A. Hydrophones

The first hydrophone dataset is from a deployment by the National Oceanic and Atmospheric Administration (NOAA) Pacific Marine Environmental Laboratory (PMEL) at Ocean Station Papa (OSP, 50.25 N, 145.13 W), south of the Gulf of Alaska. The location is very remote, around 1000 km from the Alaska and Canada mainlands, and in deep water (4250 m depth), with the hydrophone at 500 m depth, which is above critical depth. Data were processed for October to December 2018. These data include eight analysis frequency bands, with center frequencies from 127 Hz to 1.7 kHz, with 5 kHz sample rate.

The second and third hydrophones are offshore of southwest Canada, deployed and managed by Ocean Networks Canada. Both are near the seafloor, and data were processed for October 2020 to December 2021. One hydrophone is the "Cascadia Basin" deployment, 202 km west of Vancouver Island, 2660 m depth (47.76 N, 127.73 W). This is below critical depth. The more nearshore hydrophone is the "Clayoquot Slope" deployment, 78 km west of Vancouver Island, at 1260 m depth (48.70 N, 126.87 W). Critical depth is not achieved at this location. The wind climate for this region is primarily alongshore, so fetch-limited conditions are not common. These data include 18 analysis frequency bands, with center frequencies from 127 Hz to 18 kHz, with 64 kHz sample rate. At most frequencies, Cascadia is modestly quieter than Clayoquot, implying that at the latter, the impact of being within the sound channel is relatively more important than any suppression of sound by bottom interaction.

Acoustic data processing

The procedure for wind noise estimation is similar for all data sets, with modifications to account for factors such as data bandwidth, hydrophone depth, and acoustic propagation characteristics. Raw hydrophone time series data were first processed using Welch's method [13] to produce spectral estimates over stationary time intervals. A Hann window was used to minimize off-frequency-bin energy leakage via spectral sidelobes [14]. Received sound levels were then estimated over analysis frequency bands spanning 100 Hz to 20 kHz. For all data sets, lower frequencies (< 100 Hz) were not processed due to elevated ambient sound levels due to shipping activity. High frequency processing cutoffs were determined based on identified low pass filter roll-off and data acquisition system noise floor.

Calibrated spectral estimates were formed from the raw spectra based on Transmission Voltage Response (TVR) curves which accompanied the data sets. The calibrated spectra were averaged over 1-min intervals and analysis band levels were derived as the linear mean of the time-averaged spectra for the analysis frequency bands (8 for OSP and 18 for ONC). For the PMEL data, this averaging was done using 1-s FFTs with 50% overlap (119 snapshots per minute, 1 Hz frequency resolution) while the ONC data was processed using 0.1s FFTs with no overlap (600 snapshots per minute, 10 Hz frequency resolution). Finally, an algorithm was developed for automated removal of wind noise contaminants based on statistical techniques for outlier removal. Outlier selection is based on signal normalization techniques and median based statistical measures [15], [16], [17].

B. Observed wind/wave parameters

The OSP hydrophone is co-located with a PMEL buoy equipped with an anemometer at 4 m elevation (Ocean Climate Station (OCS) Project Office), and an Applied Physics Laboratory / University of Washington wave buoy [18].

The ONC hydrophones are not co-located with wind/wave observations, but a number of U.S. and Canadian buoys are in the region, eight of which are used to validate input/output to/from the 'SW (southwest) Canada' wave model described in the next section.

C. Modeled wind/wave parameters

For the OSP location, we run a 1/4° hindcast with the wave model WAVEWATCH III® ("WW3", [19], [20]). The grid design of [21] is used. Wind and ice forcing for this model comes from the Navy's operational global atmospheric model, NAVGEM [22].

For the SW Canada case, we run a similar global wave model, but since the hydrophones are not far from shore, we nest a regional wave model within the global model. We use the SWAN wave model ("Simulating WAves Nearshore", [10]), at resolution between 2.5 and 2.8 km. Both models use NAVGEM winds (and ice, in case of the global model) at 0.18° resolution (Fig. 1).

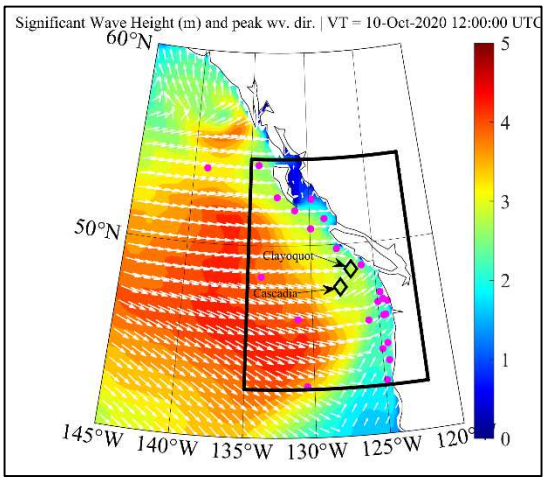

Fig. 1. Significant wave height (colors, in meters) and peak wave direction (white arrows), from the SW Canada SWAN model. Valid time is 2020 Oct. 10 12:00 UTC. The ONC hydrophones are indicated with black diamonds. Magenta dots indicate metocean buoys deployed by NOAA's National Data Buoy Center and Environment Canada. The west and south edges of the grid receive boundary forcing from WW3.

WW3 and SWAN are both phase-averaged wave models which take inputs such as 10-m wind vectors and use them to predict directional wave spectral density, as a function of space, time, frequency, and direction. From the spectra, wave parameters can be derived. They account for the effects of spatially and temporally varying winds (i.e. increasing, falling, turning) on wave growth, dissipation effects such as that by breaking, bottom friction, and interaction with sea ice, and advection in all dimensions, making them much more sophisticated (and complex) than a parametric model based on time/space averaged wind speed and approximated fetch.

D. Co-locations

In the case of OSP observed wind/wave parameters, geographic position of hydrophone data is already co-located. In all cases of model wind/wave parameters, bilinear interpolation is used for geographic co-location.

Temporal co-locations are made by taking the wind/wave parameters at 30-minute intervals, and for each temporal data point, finding the AN data within ±15-minutes of the wind/wave time, and averaging that AN data. For the OSP case, this results in up to 4250 co-locations per frequency. For ONC cases, there would be 21,100 co-locations without data gaps, but each case did contain gaps, so there were 13,300 co-locations per frequency for Cascadia and 10,900 co-locations per frequency for Clayoquot. With OSP counted twice, since observed and modeled wind/wave parameters are available, the total number of co-locations per frequency is 681 days.

IV. De-correlation analysis

Ambient noise is created by bubbles, which are created by breaking waves, and the wave energy is generated by wind action. Thus, the AN is strongly correlated with wind speed, and so models such as [4] and [9] have had success. The direct correlation between AN and wave parameters (e.g. [1]) is difficult to interpret, because much of that AN-to-wave correlation is via mutual correlation with wind speed, which is already used in the AN predictive model. One method to anticipate the potential of wave parameters for improving the prediction is to perform analysis while controlling for this mutual correlation. We have done this using two independent methods, which are described in the two sections following.

A. Band-normalized wave parameters

Fig. 2 shows examples from the (a) OSP observations and (b) Clayoquot (ONC) model output at a middle frequency, 841 Hz. The color scale here is the wave parameter m_3, normalized by the mean m_3 in a wind speed bin of width 1 m/s. Horizontal black lines indicate these bins, and the mean AN in the bin, and thus these black lines are an example of a AN prediction that is based on wind speed alone.

These plots indicate that at higher wind speeds, there is little variation of AN from the black horizontal lines. This indicates that a "wind speed only" prediction of AN is already quite accurate, and little can be done to improve upon it. At lower wind speeds, there is much more scatter above and below the black lines, indicating that some improvement is possible over the "wind speed only" model. The colors indicate that where observed AN is higher than the "wind speed only" model, normalized m_3 tends to be higher (red and orange), and below the line, the opposite is true (blue colors). This indicates that some improvement can be made on the "wind speed only" model by incorporating m_3 into the prediction model.

A limitation of this type of diagram is that it only presents results for a single wave parameter and single acoustic frequency at a time.

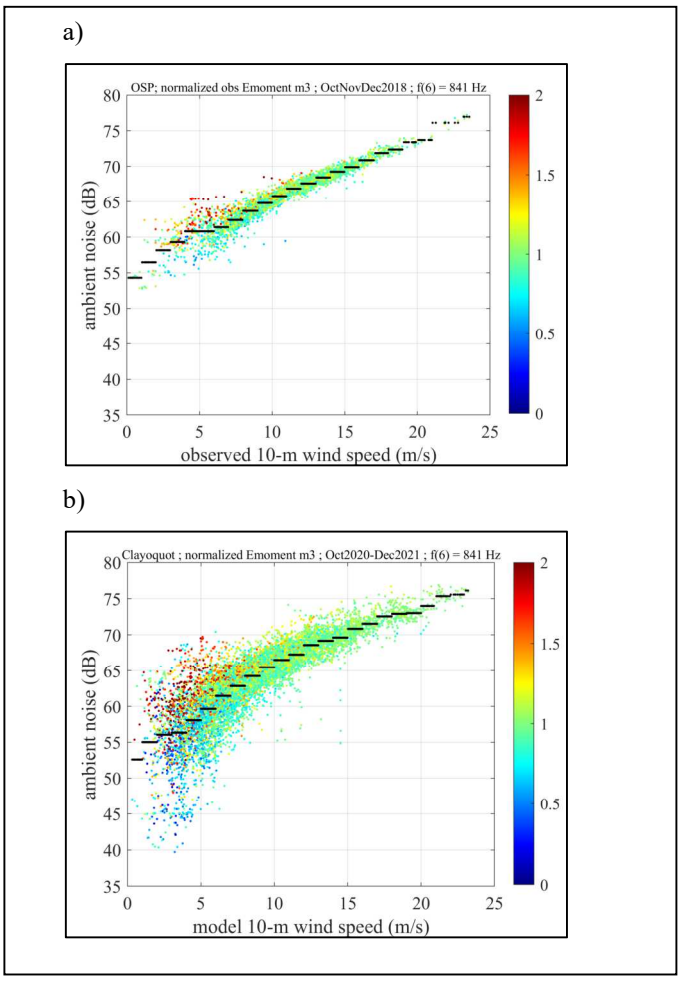

Fig. 2. AN at 841 Hz as a function of wind speed U_{10}; colors indicate the value of normalized m_3 as described in the text. Panel (a) shows results for the OSP case. Panel (b) shows results for the Clayoquot case.

B. Correlation of residuals

Another method to anticipate the potential of wave parameters for improving the prediction is to remove the component of the AN signal that correlates with the wind. Any remaining correlation is the "residual correlation".

First, we create a "wind speed only" prediction of AN for the dataset. Here, the population is split up into overlapping wind speed bins of width 1 m/s, and within each bin, a polynomial fit on frequency space is performed. Subsequently, the residual is computed as the misfit (or error) between the predicted and observed ambient noise. Having obtained the residuals, we are able to present all frequencies in the same plot: Fig. 3 shows the results for the wind speed band 4.2 to 5.2 m/s for the Clayoquot case. In panel (a) of Fig. 3, we see that the residual does not correlate with wind speed ($R_P = -0.01$), i.e. the decorrelation is successful. In panel (b), we find that correlation of the residual with the wave parameter m_4 is significant but not large, $R_P = -0.42$.

In Fig. 4, we plot the correlation vs. wind speed for several wind/wave parameters. This is the correlation with the wind speed correlation removed, and the result for wind speed is included as a thick blue line, both to indicate that the de-correlation has succeeded (low correlation), and to indicate the range in which correlation can be considered insignificant (equal to or smaller than thick blue line). A negative value indicates that a predictive model based on wind speed alone will have signed mismatch (error) that correlates negatively with the parameter in question (e.g. tendency for underprediction of AN for cases of larger m_3). Parameters are summarized here: 1) "BFI" is the "Benjamin-Feir Index" sometimes used to predict the probability of rogue waves (for this and other definitions, the reader is referred to [23]; 2) "DSPR" is a metric for directional spread of the wave spectrum; 3) "FSPR" is a metric for frequency spread of the wave spectrum; 4) "PDIR" is peak wave direction (which may correlate with breaking due to proximity to coast line); 5) "QP" is associated with frequency width and wave groupiness ; 6) "STEEP" is the H_{sig}/L, where L is mean wavelength ; 7) "WD_deg" is wind direction; 8) "precip" is mean precipitation; 9) "mm1" is the spectral energy moment m_{-1}, 10) "m0" is the moment m_0, etc.

This figure indicates that parameters such as m_2, m_3, m_4, steepness, and integrated dissipation can help to improve the AN

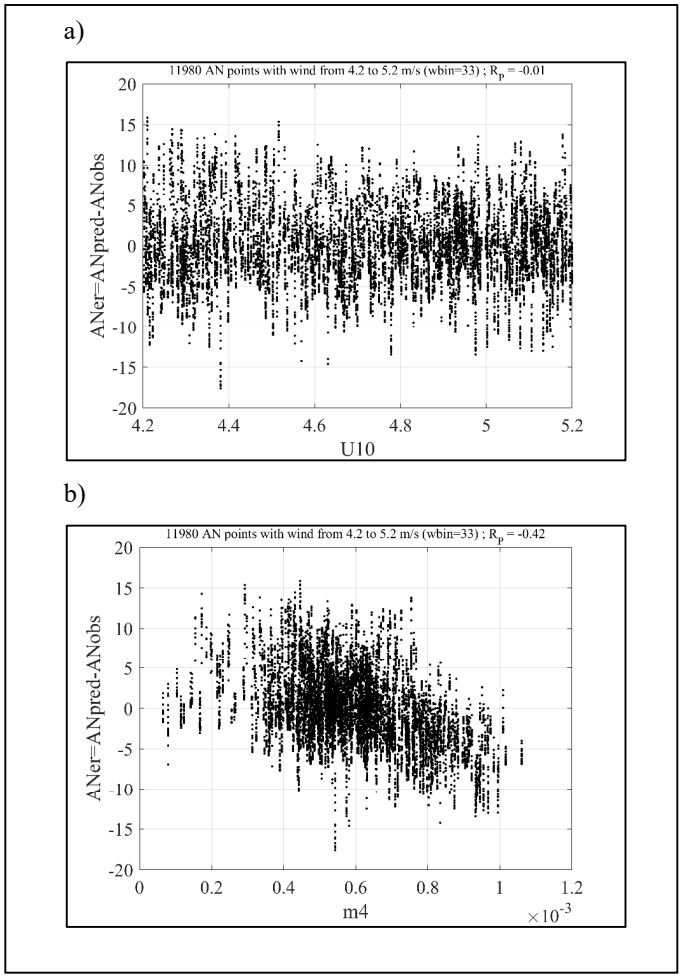

Fig. 3. Distribution of AN residual vs. wind/wave parameter for Clayoquot case, for the wind speed band of 4.2 to 5.2 m/s. In panel (a), dependency on wind speed is shown. In panel (b), dependency on m_4 is shown.

prediction, by a modest amount (correlation around 0.4), at lower wind speeds (3 to 6 m/s). At middle wind speeds (e.g. 6 to 10 m/s), this benefit is significant but smaller (correlation around 0.2). There is significant correlation with precipitation, even at higher wind speeds.

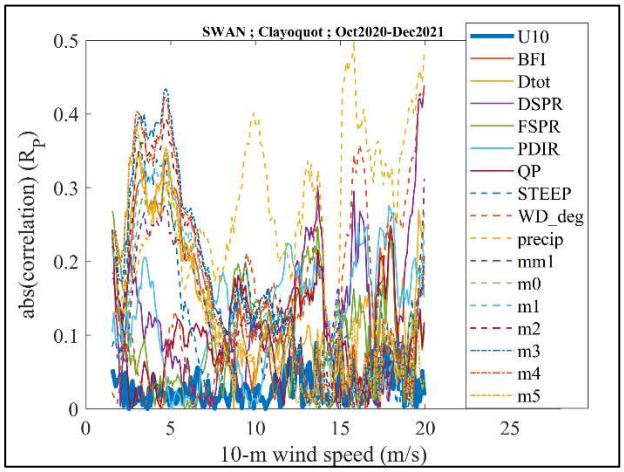

Fig. 4. Clayoquot case: Pearson correlation coefficient as a function of wind speed, for different wind/wave parameters. This is the correlation value after the correlation with wind speed has been removed (see text).

V. Multi-linear Regression

For each location, we perform linear regression to fit individual wind/wave parameters to AN and multi-linear regression to fit multiple parameters (e.g. wind speed plus one to five wave parameters). For each regression, we create both a linear fit, e.g. AN=coefficient1 × parameter1 + coefficient2 × parameter2 + .., and a log fit, e.g. AN=coefficient1 × log10(parameter1) + coefficient2 × log10(parameter2) + ..., and select the one with higher skill. We also experimented with power fits, but those results are not presented here.

For the OSP dataset, the months of October and December 2018 are used for training and November 2018 is used for prediction and evaluation. In the ONC cases, the AN time series is segmented by "day of month" over the 14-month time series. The division is at "day of month" of 21, so that ~67% of data are used for creating the regression, and ~33% of data are used for prediction and evaluation.

Unlike the works such as [4] and [9], our goal here is *not* to create a predictive model that can be applied to other locations. Our predictions do not control for sensor depth as in [9], or water depth as in [4]. The predictive models created are thereby tied to their geographic positions. Our goal, rather, is to quantify the impact of inclusion of wave parameters in model predictive skill.

Fig. 5 shows an example evaluation of the multi-linear predictions, for the Clayoquot case. The vertical axis is the RMS error of the AN prediction, in dB. We find that there is consistent but modest improvement in the predictive skill, relative to the "wind speed only" model. The degree of improvement is mostly insensitive to the selection of wave parameters.

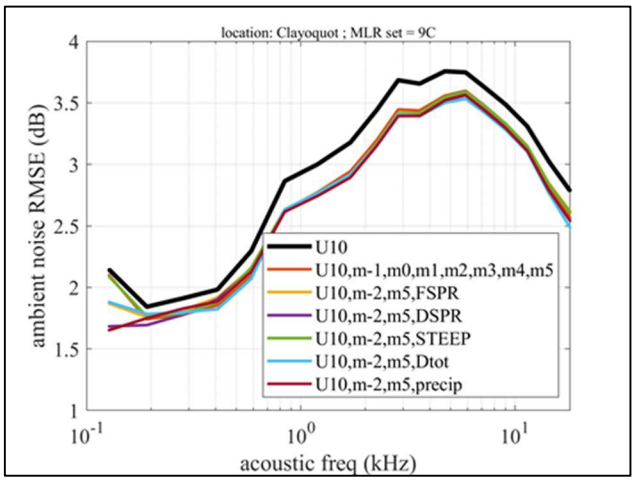

Fig. 5. RMS error in dB for prediction of AN for the Clayoquot case, using different combinations of wind/wave parameters as inputs to the AN prediction, which is based on multi-linear regression.

VI. Discussion: Limitations and Future Work

Non-local AN generation is not addressed here. Past studies have, to our knowledge, also omitted this. In principle, this can be addressed with an acoustic propagation model, but the calibration process would become prohibitively complex.

Datasets that we have used so far are not fetch-limited, climatologically speaking. This implies that locally-generated waves are often in a mature state, which in turn implies that the windsea portion of the wave spectrum is, for the most part, adequately described using information about wind speed alone. This is expected to have a strong impact on our conclusions (i.e., conclusions here are likely site-specific). Work is now underway to apply similar methods to several "High-frequency Acoustic Recording Package" (HARP) deployments of [9]), some of which are likely to be fetch-limited much of the time.

VII. Conclusions

We conclude the following, based on results presented. Discussion points are set apart using brackets []:

- Likely, the wave process which leads to ambient noise (wave breaking, bubbles) reaches a mature state more quickly than, for example, wave height. [This implies that there is less penalty for using "wind only" prediction of AN than for using "wind only" prediction of wave height.]
- The correlation study indicates a clear correlation of AN with wave parameters, independent of mutual correlation with wind. Unfortunately, at the three locations investigated, this "residual correlation" is less than 0.5.
- Potential for improving AN prediction is greatest for lower winds (e.g. 2.5-7.0 m/s).
- By including wave parameters in prediction (rather than wind speed alone), using multilinear regression: there is consistent and robust improvement in skill. However, it is modest at the three locations investigated, e.g. 0.1-0.25 dB in the RMSE.

We also make the following conclusion which are based on comparisons which are omitted from this manuscript for sake of brevity:

- The residual correlation with wave parameters is higher for lower acoustic frequencies. [This may be an indication of more remotely generated AN.]
- In our evaluations of RMSE for the OSP case (similar to Fig. 5), we get significantly higher skill (up to around 0.5 dB) using input from observations (wind only or wind and waves) relative to using model values of the same. This indicates that accuracy (or lack thereof) of the winds is a primary determiner of AN predictive skill for all cases.
- We found that prediction of AN from wind/wave parameters using Machine Learning exhibits less skill than the simpler method of multilinear regression.

Acknowledgments

We are grateful that all observational data used in this study is provided free to the research community, and acknowledge the significant effort and resources required to make this available. We thank NOAA's PMEL and Ocean Networks Canada for the hydrophone dataset; APL/UW (Jim Thomson and others) for the OSP wave buoy dataset; and NOAA PMEL (Meghan Cronin and others) for the OSP meteorological dataset. This work was funded by the Office of Naval Research through the NRL Core Program, Program Element 0602435N, Work Unit 6C32, Task Area UW-435-025. The NRL Core 6.2 project is "Ambient noise prediction using wave models". This paper is contribution NRL/PO/7320-23-5966 and has been approved for public release.

References

[1] Felizardo, F.C. and W.K. Melville (1995), Correlation between ambient noise and the ocean surface wave field *J. Phys. Oceanogr.,* **25** 513-532.

[2] Babanin, A.V. (2011), *Breaking and Dissipation of Ocean Surface Waves*, Cambridge Univ. Press, 463 pp.

[3] Knudsen, V.O., R.S. Alford, and J.W. Emling (1948), Underwater ambient noise, *J. Mar. Res*., 7, 410-429.

[4] Wenz, G.M., (1962), Acoustic Ambient Noise in the Ocean: Spectra and Sources, *The Journal of the Acoustical Society of America* 34, 1936-1956 https://doi.org/10.1121/1.1909155

[5] J. H. Wilson, Low-frequency wind-generated noise produced by the impact of spray with the ocean's surface, Journal of the Acoustical Society of America 68, 952 (1980); doi: 10.1121/1.384783.

[6] Prosperetti, A. (1988), Bubble-related ambient noise in the ocean, *The Journal of the Acoustical Society of America* 84, 1042-1054, https://doi.org/10.1121/1.396740.

[7] H. Medwin and A. C. Daniel, Acoustical measurements of bubble production by spilling breakers, Journal of the Acoustical Society of America, 88, 408 (1990), doi: 10.1121/1.399917.

[8] Farmer, D. M., and Vagle, S. (1988), On the determination of breaking surface wave distributions using ambient sound, *J. Geophys. Res.*, 93(C4), 3591– 3600, doi:10.1029/JC093iC04p03591.

[9] J A. Hildebrand, K. E. Frasier, S. Baumann-Pickering, and S. M. Wiggins, An empirical model for wind-generated ocean noise, Journal of the Acoustical Society of America 149, 4516 (2021); doi: 10.1121/10.0005430

[10] Booij, N., Ris, R. C. and Holthuijsen, L. H., 1999. A third-generation wave model for coastal regions, Part 1: Model description and validation. *J. Geophys. Res*., 104 (C4), 7649-7666.

[11] Phillips, O.M., 1966: Dynamics of the Upper Ocean, Cambridge at the University Press, 261pp.

[12] Babanin, A.V., and I.R. Young, 2005: Two-phase behaviour of the spectral dissipation of wind waves, Proc. Ocean Waves Measurement and Analysis, Fifth Intern. Symposium WAVES 2005, 3-7 July, 2005, Madrid, Spain, Eds. B. Edge and J.C. Santas, paper no.51, 11 pp.

[13] P. Welch, The use of fast Fourier transform for the estimation of power spectra: A method based on time averaging over short, modified periodograms, IEEE Transactions on Audio and Electroacoustics, vol. 15. no. 2, pp. 70 – 73 1967.

[14] F. J. Harris, On the Use of Windows for Harmonic Analysis with the Discrete Fourier Transform, Proc. IEEE, vol. 66, pp. 51 – 83, Jan. 1978.

[15] J. E. Summers, "Design of a signal normalizer for high-clutter active-sonar detection," J. Acoust. Soc. Am. 143, 1760 (2018)

[16] P. J. Rousseeuw and C. Croux, "Alternatives to the Median Absolute Deviation," Journal of the American Statistical Assoc., December 1993, Vol. 88, No. 424.

[17] F. Schwock and S. Abadi, "Characterizing underwater noise during rain at the northeast Pacific continental margin," J. Acoust. Soc. Am. 149 (6), June 2021, pp. 4579 – 4595.

[18] Thomson, J., Talbert J., de Klerk, A., Brown, A., Schwendeman M., Goldsmith, J., Thomas, J., Olfe, C., Cameron, G. and Meinig, C. (2015). Biofouling effects on the response of a wave measurement buoy in deep water. *J. Atm. Ocean. Tech*., 32, 1281-1286, doi: 10.1175/JTECH-D-15-0029.1.

[19] Tolman, H.L., 1991. A Third-generation model for wind-waves on slowly varying, unsteady, and inhomogeneous depths and currents, *J. Phys. Oceanogr.* **21**(6)*,* 782-797.

[20] The WAVEWATCH III® Development Group (WW3DG), 2019. User manual and system documentation of WAVEWATCH III® version 6.07. *Tech. Note 333*, NOAA/NWS/NCEP/MMAB, College Park, MD, U.S.A., 465 pp. + Appendices.

[21] Rogers, W.E. and R.S. Linzell, 2018. The IRI Grid System for Use with WAVEWATCH III. *NRL Report NRL/MR/7320--18-9835*, 47 pp. [available from www7320.nrlssc.navy.mil/pubs.php]

[22] Hogan, T., and 16 Coauthors, 2014. The Navy Global Environmental Model. *Oceanogr.,* **27**(3), 116-125.

[23] SWAN team, 2019. SWAN User Manual, SWAN Cycle III version 41.31, Delft University of Technology, swan.tudelft.nl , 135 pp.